Equilibrium reconstruction of local shear in the pedestal on ASDEX Upgrade.

P.J. Mc Carthy,[1] M.G. Dunne,[1] R. Fischer,[2] J.C. Fuchs,[2] L. Giannone,[2]
W. Suttrop,[2] E. Viezzer,[2] E. Wolfrum,[2] and The ASDEX Upgrade Team[2]

[1] *Department of Physics, University College Cork, Association Euratom-DCU, Cork, Ireland.*

[2] *Max Planck Institut für Plasmaphysik, Boltzmannstrasse 2, D-85748 Garching, Germany*

Introduction

Equilibrium magnetic measurements ("magnetics") outside the plasma provide essential information, including the identification of the plasma boundary surface, for MHD equilibrium reconstruction on tokamaks and other magnetically confined plasma experiments. A recent paper [1] has shown that long-accepted assumptions about the limitations of recovering information on the internal current density profile from magnetics were pessimistic, and that together with global parameters consisting of the plasma current I_p, β_{pol} and l_i, additional moments of the toroidal current density j_ϕ, strongly localized in the edge region of the plasma, are recoverable from magnetics when the plasma is bounded by a separatrix. This identifiability in the edge region also applies to any derived equilibrium quantities. Local magnetic shear, which is a measure of the rate at which initially adjacent field lines on neighbouring flux surface separate with distance advanced along the field lines, is a structural property of magnetic fields that has an important influence on plasma stability. Defining the unit vector $\boldsymbol{e}_\perp = \boldsymbol{e}_\psi \times \boldsymbol{b}$ where $\boldsymbol{b} = \boldsymbol{B}/B$ is the local magnetic field direction and $\boldsymbol{e}_\psi$ is the local unit normal to the flux surface, local shear defined as $S_\ell = -\boldsymbol{e}_\perp \cdot \nabla \times \boldsymbol{e}_\perp$ (this definition is based on [2]) was evaluated for axisymmetric equilibria to yield an exact expression in terms of standard equilibrium code outputs [3]:

$$S_\ell = \frac{F}{R^4 B_\theta^2 B^2}\left\{(\psi_{RR} - \psi_{ZZ})(\psi_R^2 - \psi_Z^2) + 4\psi_R\psi_Z\psi_{RZ}\right\} + \frac{F\psi_R}{R^3B^2} - \frac{F' B_\theta^2}{B^2} \qquad (1)$$

where $\psi_R = \partial\psi/\partial R$, etc. This expression for the local magnetic shear, valid for an axisymmetric MHD equilibrium of arbitrary poloidal cross-section and aspect ratio, can be shown [3] in the limit $R/a \to \infty$ and circular flux surfaces to be related to the common expression for global shear, $s = (r/q)dq/dr$, by $S_\ell = s/L_c$ where $L_c = qR$ is the connection length.

Experimental examples from ASDEX Upgrade

As an illustration, we present contour plots of the local shear for ASDEX Upgrade standard H-mode discharge 28349 ($I_p = 1\,\mathrm{MA}$, $B_t = -2.5\,\mathrm{T}$, $\bar{n}_e = 8.9\times10^{-19}\,\mathrm{m}^{-3}$) for which the evolution of relevant parameters in the current flat-top time window $1.2\,\mathrm{s} \le t \le 2.7\,\mathrm{s}$ is plotted in fig. 1.

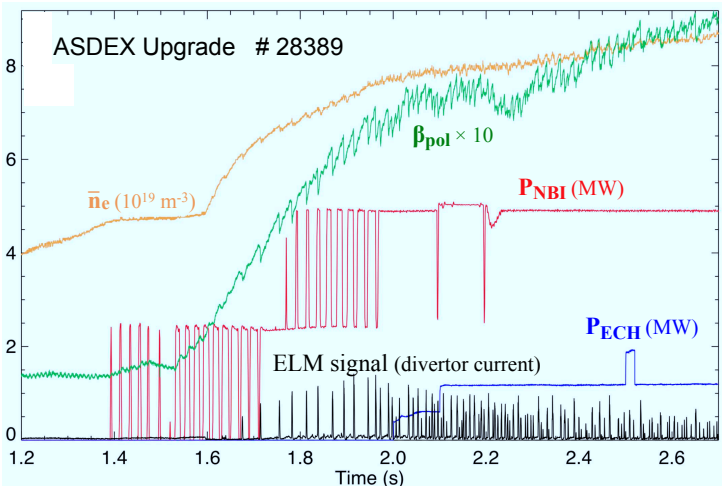

FIG. 1: Line-averaged density (ochre), poloidal beta (green), neutral beam (red) and electron cyclotron (blue) heating powers and the divertor current ELM signal (black) for ASDEX Upgrade discharge 28389 ($I_p = 1\,\mathrm{MA}$, $B_t = -2.5\,\mathrm{T}$, $\bar{n}_e = 8.9 \times 10^{-19}\,\mathrm{m}^{-3}$) for $1.2\,\mathrm{s} \le t \le 2.7\,\mathrm{s}$. The first ELM occurs at $t = 1.676\,\mathrm{s}$.

Figure 2 shows a sequence of contour plots of $S_\ell(R, Z)$ evaluated using equation (1) from a

sequence of equilibria constrained by equilibrium magnetic data, divertor tile current measurements, edge kinetic profiles and axial safety factor ≈ 1.0 using the CLISTE equilibrium reconstruction code [1]. Each time point was selected to be at the end of the ELM recovery phase [4]. The first time point at $t = 1.4\,\mathrm{s}$ lies in the ohmic phase of the discharge, The second, at $t = 1.62\,\mathrm{s}$ is $\approx 50\,\mathrm{ms}$ before the first ELM. The third, at $t = 1.70\,\mathrm{s}$ is 25 ms after the first ELM (but before the second) and the fourth time point, $t = 2.62\,\mathrm{s}$, lies in a well-heated phase of the discharge ($\beta_{pol} \approx 0.86$). Red regions indicate negative and green positive local shear, and because of the choice of plotting function used (of type Tanh[1/x]), the darkest hues occur at zero crossings while the lightest occur at extrema.

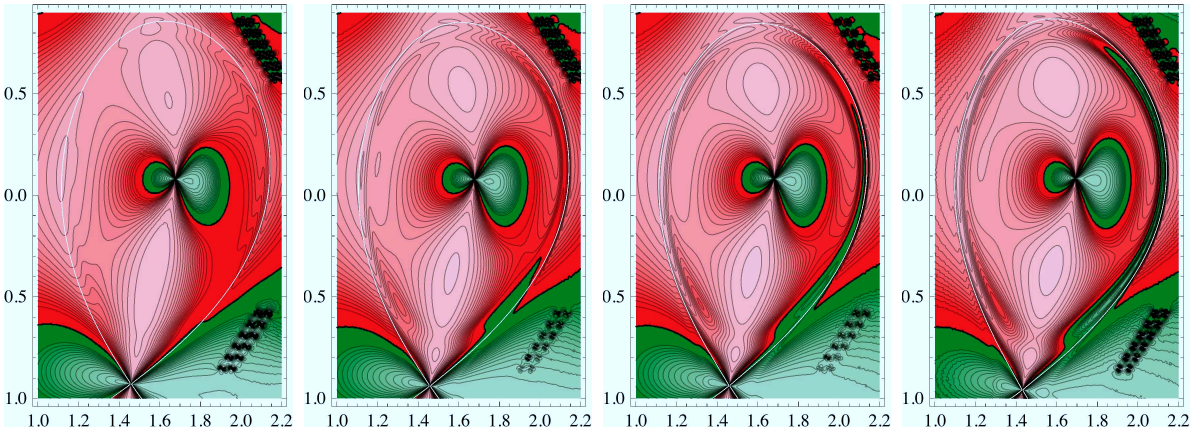

FIG. 2: Sequence of local shear contour plots for ASDEX Upgrade discharge 28389 for (left to right) $t = 1.40\,\mathrm{s}$, $t = 1.62\,\mathrm{s}$, $t = 1.70\,\mathrm{s}$, $t = 2.62\,\mathrm{s}$ calculated from CLISTE equilibrium reconstructions. These time points correspond to ohmic, pre-first ELM, post-first ELM and during a well-heated phase of the discharge (see figure 1). Red indicates negative and green positive local shear, and the darkest hues occur at zero crossings. The separatrix is plotted as a white curve. See [3] for more details.

The most striking feature of the plot sequence is the growth with β_{pol} of a narrow radial region of positive shear just inside the outboard separatrix. Starting in the lower outboard quadrant, the positive shear region first crosses the midplane at a time separated by the order of 10 ms from the occurrence of the first ELM, which we investigate below. With increasing β_{pol}, the region of positive S_ℓ broadens radially and extends poloidally upwards, while remaining confined to the outboard side. The asymmetric figure-of-eight region of positive shear centered on the magnetic axis and present on all plots was shown in [3] to be a consequence of ellipticity.

Given the pattern of local shear reversal in the pedestal region at the occurrence of the first ELM, it is interesting to consider the corresponding behaviour of the poloidal current density profile, recently proposed as a critical quantity in discriminating between plasma regimes [5] and as a mechanism for phase transitions [6]. CLISTE output includes error bars for the fitted $p'(\psi)$ and $FF'(\psi)$ source profiles calculated from the variance-covariance matrix of the linear regression which determines the set of free parameters at the cycle where the convergence criterion is met [1]. Error bars for related quantities such as the poloidal current density profile $j_\theta = F'B_\theta/\mu_0$ are easily constructed. Figure 3 shows the outboard magnetic midplane profile $j_\theta(R,\, Z_{mag.\,axis})$ with 1σ error bars (blue traces) for the four time points in figure 2. Also plotted (red trace) is the local shear midplane profile $S_\ell\,(R,\, Z_{mag.\,axis})$. The evolution of the two profiles is closely correlated, in particular the S_ℓ profile increases through zero at the same radial location, within 1σ error bars, as j_θ for the post-first ELM time points $t = 1.7\,\mathrm{s}$ and $t = 2.62\,\mathrm{s}$. Note that j_θ is already weakly positive for the pre-first ELM time point $t = 1.62\,\mathrm{s}$. In this discharge, the L-H transition occurs at $t = 1.59\,\mathrm{s}$ (see following section). The last term in equation (1) for S_ℓ has a direct dependence on j_θ through the presence of the factor F' and hence it might be

assumed that this term explains the similar evolution of j_θ and S_ℓ. Its magnitude, however, is negligible in the pedestal region ($|F'B_\theta^2/B^2| \approx 0.01$) and instead it is the temporal evolution of ψ_{RR} that determines the development of the sign reversal in S_ℓ in the pedestal, as can be seen from the green and magenta traces in figure 3 which represent a partitioning of S_ℓ into the ψ_{RR}-dependent term $(F/(R^4B_\theta^2B^2))\psi_{RR}(\psi_R^2 - \psi_Z^2)$ (green trace) and all other terms in equation (1) (magenta trace). Both traces are monotonic in the pedestal region for the ohmic time point $t = 1.4\,\mathrm{s}$. Thereafter the magenta trace, which includes the term $-F'B_\theta^2/B^2$, remains almost monotonic, but the green trace develops a prominent local maximum 2 cm inside the separatrix which accounts for the sign reversal in S_ℓ.

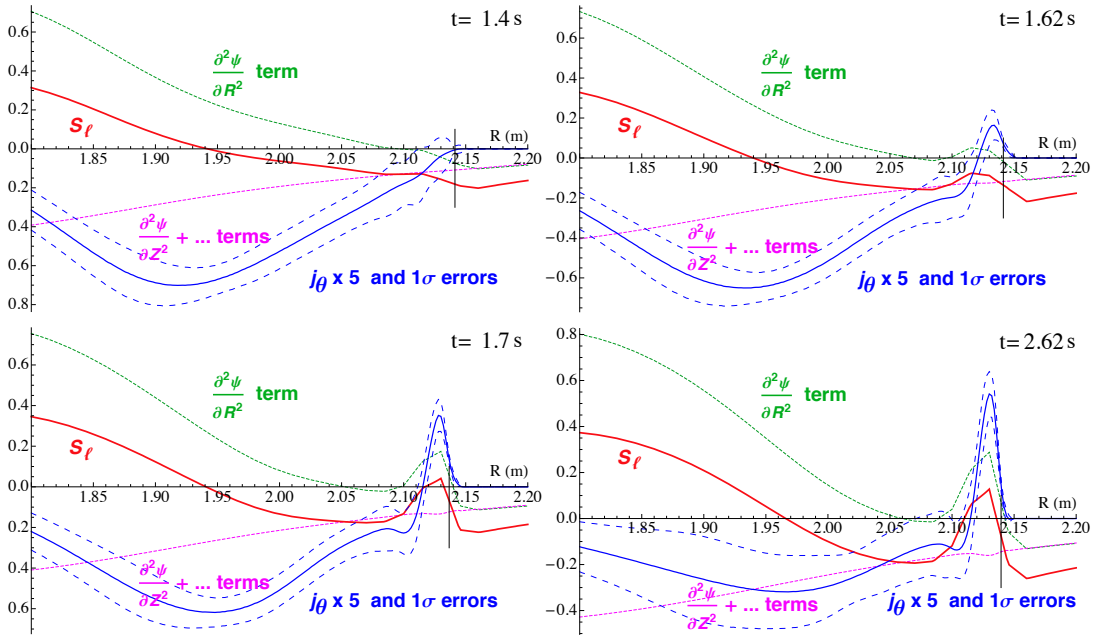

FIG. 3: Sequence of outboard magnetic midplane profiles of local shear components (units: m^{-1}) and poloidal current density $\times 5$ (units: $\mathrm{MA/m^2}$) versus major radius for ASDEX Upgrade discharge 28389 and the time points shown in fig. 2. The green dotted trace is the expression $(F/(R^4B_\theta^2B^2))\psi_{RR}(\psi_R^2 - \psi_Z^2)$. The magenta trace consists of all other terms in equation (1). The red trace, the sum of the green and magenta traces, is the local shear. The blue traces consist of the poloidal current density (solid) and 1σ error bars (dashed). The thin line at $R \approx 2.14\,\mathrm{m}$ marks the separatrix location.

Investigation of zero crossings of j_θ and the local shear S_ℓ in the pedestal.

To investigate more closely the proximity to the 1st ELM of zero crossings in the pedestal for both the local shear and the poloidal current density profile, an initial study of 10 ELMy discharges, chosen for good quality edge kinetic profiles [7] and a variety of edge conditions, was carried out based on high spatial resolution CLISTE reconstructions constrained by magnetics, edge kinetics and SOL currents with ELM crash time points excluded. A good example of the typical relationship found between $t_{\mathrm{L\to H}}$, $t_{j_\theta \nearrow 0}$, $t_{S_\ell \nearrow 0}$ and $t_{\mathrm{1st\ ELM}}$ is provided by ASDEX Upgrade discharge 28847 where fig. 4 shows time traces of S_ℓ (red) and j_θ (blue) evaluated at the location of maximum pedestal pressure gradient, with other traces as labelled in the caption. The j_θ zero crossing occurs within ≈ 1 ms of the $L \to H$ transition while S_ℓ goes positive in the window $t_{\mathrm{L\to H}} < t < t_{\mathrm{1st\ ELM}}$. There is a clear pattern of recovery in j_θ and S_ℓ following each type I ELM. In contrast to the behaviour of S_ℓ, the global shear, calculated by flux surface integration of eq. (1), does not make a zero crossing. This was the case for all 10 discharges (26313, 26910, 27963, 28216, 28245, 28389, 28847, 29924, 29926, 29986) in this study. Summary statistics for various relative times (where $\mathrm{t_a \to t_b}$ is synonymous with $\mathrm{t_b - t_a}$) are presented in tabular form below, where all quantities are rounded to the nearest ms.

TABLE I: Summary statistics for 10-discharge study

	mean	std. deviation	minimum	maximum
$t_{j_\theta=0} \rightarrow t_{\mathrm{L}\rightarrow\mathrm{H}}$	3	7	-11	15
$t_{j_\theta=0} \rightarrow t_{S_\ell=0}$	34	31	5	104
$t_{\mathrm{L}\rightarrow\mathrm{H}} \rightarrow t_{S_\ell=0}$	32	33	3	101
$t_{S_\ell=0} \rightarrow t_{\mathrm{1st\ ELM}}$	57	56	-22	145
$t_{\mathrm{L}\rightarrow\mathrm{H}} \rightarrow t_{\mathrm{1st\ ELM}}$	90	36	36	148

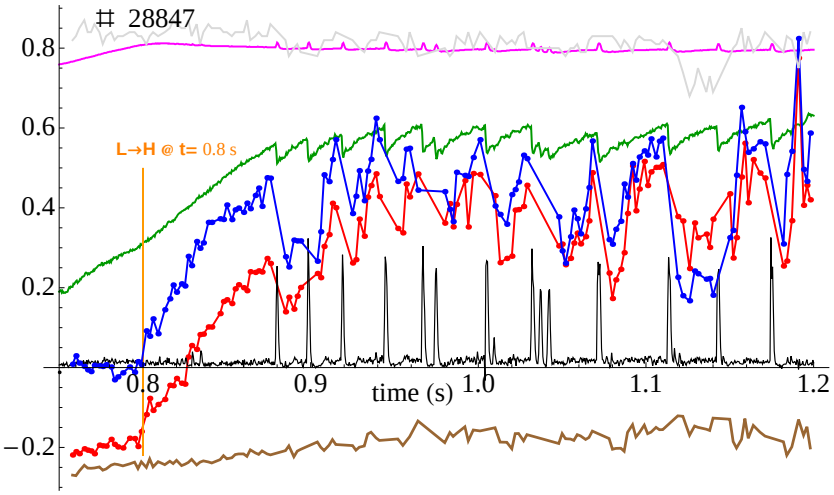

FIG. 4: ASDEX Upgrade # 28847: Time traces of **local shear** S_ℓ $\times 2$ **(m^{-1})**, $j_\theta \times 10$ (MA m^{-2}), **global shear/L_c (m^{-1})**, β_{pol}, I_p (MA), $10(\rho_{\nabla p_{max}} - 0.9)$, **ELM signal**. All profile quantities, obtained from high resolution CLISTE interpreted equilibria, were evaluated at the location of the maximum pedestal pressure gradient $\rho_{\nabla p_{max}}$ which remained at $\rho_{pol} \approx 0.98$ over the analysis window.

Summary and discussion

The exact expression for axisymmetric local shear S_ℓ derived in [3] and now incorporated in CLISTE [1] has been applied to a set of 10 ASDEX Upgrade discharges with well-diagnosed pedestals, where it was found in all cases that a zero crossing of S_ℓ at the location of maximum pressure gradient occurs $\approx 30 \pm 30$ ms following the L-H transition and $\approx 60 \pm 60$ ms prior to the first type I ELM. However, the salient result from the present work concerns not the local shear itself, but the very close correlation between the zero crossing of the poloidal current profile in the pedestal and the L-H transition. For the 10 discharges studied here, $j_\theta \rightarrow 0$ occurs on average 3 ms prior to the L-H transition with a standard deviation of 7 ms. These preliminary results support the hypotheses in [5, 6] where it is proposed that $j_\theta = 0$ is the necessary condition for an L-H transition. A more comprehensive investigation of the foregoing questions is planned for the coming period.

Acknowledgements

The first author is indebted to Francois Ryter (IPP) for assistance in identifying L-H transitions. This work was supported by a research agreement between the Max Planck Institut für Plasmaphysik, Garching and the Department of Physics, University College Cork, and by EURATOM.

[1] P J Mc Carthy and ASDEX Upgrade Team, Plasma Phys. Control. Fusion **54** 015010 (2012).
[2] M Nadeem, T Rafiq and M Persson, Phys. Plas, **8** 4375 (2001).
[3] P J Mc Carthy and ASDEX Upgrade Team, Plasma Phys. Control. Fusion **55** 085011 (2013).
[4] M G Dunne *et al.*, Nucl. Fusion **52** 123014 (2012).
[5] J Garcia and G Giruzzi, Phys. Rev. Lett. **204** 205003 (2010).
[6] E R Solano and R D Hazeltine, Nucl. Fusion **52** 114017 (2012).
[7] R Fischer and R Dinklage Rev. Sci. Instr.. **75** 4237-39 (2004).